Impact of carrier dynamics on the photovoltaic performance of quantum dot solar cells

Impact of Carrier Dynamics on the Photovoltaic Performance of Quantum Dot Solar Cells

Mariangela Gioannini[1], *Ariel P. Cedola*[2], *and Federica Cappelluti*[1]

[1]*Department of Electronics and Telecommunications, Politecnico di Torino, Corso Duca degli Abruzzi 24, 10129 Torino, Italy*

[2]*GEMyDE, Group of Studies about Materials and Electronic Devices, Faculty of Engineering, National University of La Plata, Argentina.*

E-mail: federica.cappelluti@polito.it

ABSTRACT

The paper presents a theoretical investigation of the impact of individual electron and hole dynamics on the photovoltaic characteristics of InAs/GaAs quantum dot solar cells. The analysis is carried out by exploiting a model which includes a detailed description of QD kinetics within a drift-diffusion formalism. Steady-state and transient simulations show that hole thermal spreading across the closely spaced QD valence band states allows to extract the maximum achievable photocurrent from the QDs; on the other hand, slow hole dynamics turns QDs into efficient traps, impairing the short circuit current despite the extended light harvesting provided by the QDs.

I. INTRODUCTION

The use of quantum dots (QDs) in III-V solar cells is an attractive technology to enhance the power conversion efficiency of single- and multi-junction solar cells through bandgap and carrier dynamics engineering. Reported InAs/GaAs QD solar cells (QDSC) have generally shown a limited improvement of the short circuit current density ($J_{\rm sc}$) together with a degradation of the open circuit voltage ($V_{\rm oc}$), that have allowed a marginal improvement, at the best, of the power conversion efficiency with respect to the bulk counterpart [1]. Recently, promising results have been demonstrated through n-type doping of QDs either in terms of $V_{\rm oc}$ recovery [2]–[4] and $J_{\rm sc}$ enhancement [5]. Such improvements rely on different and possibly concomitant mechanisms, depending also on device structure and material quality, such as the reduction of recombination through mid-gap states, the increase of sub-bandgap photogeneration and/or collection, the suppressed capture and increased carrier lifetime in the QDs. The overall scope of experimental results on both undoped and doped cells suggests that the actual device performance is the

result of a complex interplay between carrier transport processes in the host GaAs material, carrier capture in the wetting layer (WL), and carrier intersubband dynamics in the QDs.

However, while a significant amount of experimental and theoretical works has focused on the investigation of carrier dynamics in QD lasers and semiconductor optical amplifiers [6], [7], [8], less effort has been put on studying carrier dynamics in QD solar cells, with emphasis on evaluating carrier lifetime in QD states [4] and carrier escape mechanisms [9]. Capture dynamics and intersubband processes in the cell under forward bias still remain to be investigated. In QD lasers, the QD carrier dynamics is mainly driven by efficient carrier-carrier scattering processes thanks to the accumulation of carriers in the WL state [8]; this process gives different time scales for the electron and hole dynamics (with holes in general faster than electrons) and, for this reason, most of the models currently used for QD lasers include independent electron and hole rate equations to describe the desynchronized dynamics of carriers [10]. The situation is different when dealing with QD solar cells: in this case just a small density (compared to the laser case) of e-h pairs is present in the QD confined states or in the WL because of the low photogeneration rate; thus, carrier-carrier scattering cannot be considered as a driving mechanism for carrier dynamics and other physical processes, such as multiphonon interaction [11], must be called for. Finally, it is still to be understood if, in these almost empty QDs, the photogenerated electron and hole follow an independent and desynchronized dynamics supported by multiphonon processes, or if it would be more realistic assuming the dynamics of the correlated e-h pair considered as an exciton [12] [13]. Concerning QD lasers, the assumption of separate e-h dynamics or of exciton dynamics leads to quite different calculated laser performance as analysed in detail in [13].

In this contribution we present a simulation study of the photovoltaic performance of typical GaAs-based QDSCs aimed at understanding how the difference between electron and hole capture and relaxation dynamics affect the cell performance. Simulation results obtained under the hypothesis of separate electron and hole dynamics and of exciton dynamics are compared in terms of their impact on collection efficiency and open circuit voltage. The analysis is carried out by exploiting an *ad hoc* developed simulation tool that couples a drift-diffusion transport model with a detailed description of photogeneration and carrier kinetics in the QDs [14].

The paper is organized as follows: in Section II we briefly introduce the numerical model, in Section III we present and discuss the simulation results, and in section IV we draw the conclusions.

II. Model Overview

The detailed description of the modelling approach is reported in [14]; we briefly summarize here the most relevant concepts and we refer to [14] for all the details of the model equations. Fig. 1a shows the typical structure of an InAs/GaAs solar cell: N QD layers are grown in the intrinsic GaAs region between the p-type emitter and the n-type rear contact with the aim of extending the harvesting of the solar spectrum beyond the GaAs energy gap. The present formulation applies to uncoupled QD layers, wherein tunneling between QD layers is negligible. As shown in the schematic of Fig. 1b, this structure can be analysed with a 1D model that includes a drift-diffusion description of the bulk material and a set of phenomenological rate-equations (REs) for the QDs. QDs are modeled as a three-level system, including ground state (GS), excited state (ES), and WL state. The WL state, in particular,

accounts for both the continuum-like QD upper states and the actual 2-D energy state due to the thin wetting layer. The REs include the photogeneration in WL, ES and GS states, the electron and hole capture from the GaAs barrier into the WL state, the cascade relaxation process in the ES and GS, the escape to the higher energy states and the recombination in the WL and confined states. These intersubband electron and hole dynamics are modeled by characteristic scattering times (i.e. capture, relaxation and escape time constants). In general, the carrier escape from the QDs to the barrier may be promoted by three main processes, namely thermal excitation, tunneling, and infrared (IR, at intersubband wavelengths) photon absorption. At room temperature, the escape by IR optical excitation is likely negligible with respect to the thermal and tunneling processes [15]. The escape of holes, due to their shallow confinement, is essentially thermally-driven, whereas a more complex picture may underlie the electrons escape. In fact, thermal escape is usually dominant for the escape from GS, whereas tunneling can be significant for the higher energy states under high electric fields, on the order at least of a few tens of kV/cm as reported e.g. in [9,16]. Clearly, the relative strength of thermal-assisted or tunneling-assisted mechanisms on the escape rate is very dependent on the QD energy levels and device structure as well. For the relatively small QDs considered in the following discussion tunneling turns to be negligible in the assumed operating conditions. Thus, in the simulations only thermal-assisted escape has been considered. In this case, the thermal escape time constant (from state k to higher energy state j) is connected to the capture time constant by the detailed balance at thermal equilibrium:

$$\tau^{e,h}_{\mathrm{ESC},k\to j} = \frac{N^{e,h}_{\mathrm{k}}}{N^{e,h}_{\mathrm{j}}}\tau^{e,h}_{\mathrm{CAP},j\to k}\exp\left(\frac{\Delta E^{e,h}_{jk}}{k_{\mathrm{B}}T}\right). \tag{1}$$

being $N^{e,h}_{\mathrm{kj}}$ the electron/hole density of states in the j,k states, $\Delta E^{e,h}_{jk}$ the electron/hole energy separation between the two states in the conduction/valence band and $\tau^{e,h}_{\mathrm{CAP},j\to k}$ the capture (or relaxation) time constant. Capture and relaxation time constants are set in a phenomenological way, by comparison with experimental results [14].

III. Results and Discussion

Simulations were carried out on a pin stucture with 500 nm intrinsic region embedding 20 QD layers, placed in the center of the i region and equally spaced by about 23 nm. QD density per layer is $6\times10^{10}\mathrm{cm}^{-2}$. The p-type emitter is made by a 50 nm p^+ GaAs contact layer with doping density of 5×10^{18} cm^{-3} and a 100 nm p GaAs layer with doping density 1×10^{18} cm^{-3}. The 500 nm i-region is separated from the 300 nm n^+ GaAs contact layer by a 50 nm intrinsic GaAs buffer layer. A refererence bulk GaAs cell is also considered, with the same pin geometry and doping levels as above. The InAs QDs have GS absorption centered at 1.13 eV with FWHM due to inhomogenous brodening of 38 meV. Inter-level spacings [$\Delta E^{\text{B-WL}}$, $\Delta E^{\text{WL-ES}}$,$\Delta E^{\text{ES-GS}}$] are [140, 62 ,70] meV for the conduction band, and [28, 16, 16] meV for the valence band. Full details on QD structure and optical absorption spectra are reported in [14]. The bulk model accounts for radiative and Shockley-Read-Hall (SRH) recombination, and carrier velocity saturation according to the Caughey-Thomas model [17]. Standard GaAs material parameters were used [18]. In particular, 10 ns for the SRH lifetimes, and 2.0×10^{-10} cm^{3}s^{-1} for the radiative recombination rate. The energy band diagram at short circuit, under 1-sun AM1.5G illumination, is sketched in Fig. 2.

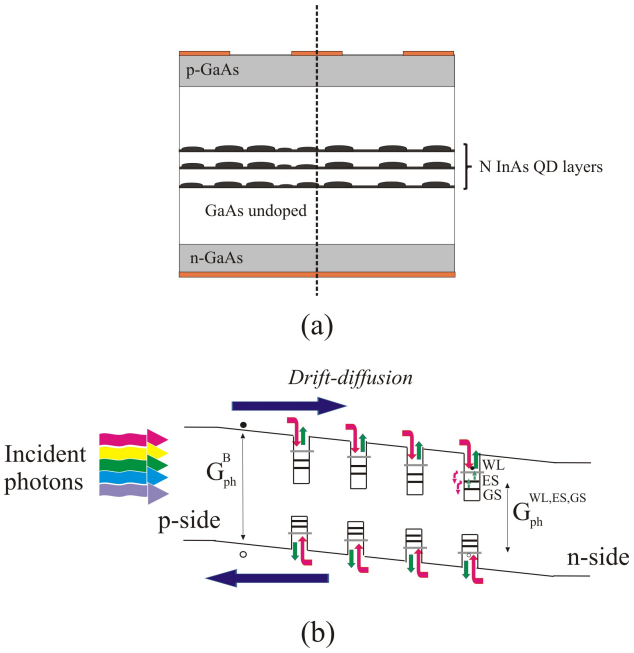

Fig. 1. (a) Sketch of the typical InAs/GasAs QDSC structure with N InAs QD layers in the intrinsic GaAs base. (b) Conceptual sketch of the 1D model (along the cutline in Fig. 1) in [14]: sun illumination is on p-side; the photo-generation in the barrier (G_{ph}^{B}) creates electron and hole pairs that move towards the contacts by drift-diffusion (blue arrows) or can be captured in the QDs (red arrows). Captured or photogenerated ($G_{\text{ph}}^{\text{WL,ES,GS}}$) QD carriers can escape to higher energy states (green arrows) or relax to lower energy states (red arrows), where they may also recombine.

We have analysed the cell performance under two different assumptions for the intersubband carrier dynamics. In the first case, we assume that intersubband electron and hole dynamics are completely uncoupled and that the hole capture and relaxation time constants (and thus also the escape times in (1)) are much faster than the electron ones [14]. We refer to this model as the *separate e-h dynamics* model. The assumption of hole dynamics faster than electron dynamics can be supported by pump-probe experiments carried out in QD-SOAs in the absorption regime [19] and therefore in an operating condition similar to the one of QDSCs, i.e. when the QDs are almost empty of carriers and carrier dynamics is not dominated by carrier-carrier scattering mechanism. Electron capture times, as extracted from experimental results [14], are assumed as 0.3 ps from bulk to WL states and 1 ps for capture from WL to ES as well as for relaxation from ES to GS states. Hole capture and relaxation time constants are assumed to occur on a scale of 0.1 ps (about one order of magnitude faster than electrons) in agreement with the results reported in [19]. In the second case, we follow a more simplified approach assuming that hole dynamics mirrors the electron dynamics (with electron time constants set as in the *separate e-h dynamics*); we refer to this model as the *exciton model* [13]. This hypothesis can also be considered as the limiting case when the hole and electron dynamics are similar, as predicted in [20] for shallow QDs. The calculated photovoltaic performance for the two case studies are summarized in Table I, where we report the J_{sc} and V_{oc} under 1-sun AM1.5G illumination, the short-circuit current density, J_{sc}^{QD}, obtained when only QD photogeneration takes place (i.e. filtering out the part of the solar

spectrum absorbed by the GaAs) and the difference, ΔJ_{sc}, between the short circuit current density of the QD cells with respect to the reference cell. The J-V characteristics calculated under different illumination conditions for the *separate e-h dynamics* model are shown in Fig. 3, together with the J-V of the reference cell. The *separate e-h dynamics* model predicts that the inclusion of the QD layers is beneficial in increasing the achievable short-circuit current: ΔJ_{sc} is positive and nearly equal to the contribution J_{sc}^{QD} evaluated under filtered sunlight. This one, in turn, is verified to be very close to the integrated QD photogeneration rate, i.e. the collection efficiency of QD photogenerated carriers is almost unitary, and the small value of J_{sc}^{QD} is due to the weak optical absorption of the QD layers [14]. This suggests that, in the *separate e-h dynamics* case, at short-circuit, all the QD photogenerated carriers can thermally escape out of the QDs and fully contribute to the short-circuit current, while capture and recombination of bulk carriers through the QDs is extremely small. In contrast, the *exciton model* predicts a reduced J_{sc} of the QD cell with respect to the reference one ($\Delta J_{sc} < 0$), even though the QD contribution only, J_{sc}^{QD}, is still significant. This points out a behavior dominated by the capture in the QDs of the photogenerated bulk carriers followed by recombination. The point is further evidenced by analyzing the amount of the different carrier loss processes taking place within the intrinsic region, according to the adopted dynamic model. To this aim, Fig. 4 reports the equivalent recombination currents, calculated by integrating the recombination in the QDs and in the GaAs across the intrinsic region, as a function of the voltage, which spans from the short circuit to the V_{oc} of each case. It is worth to note that in the present devices, recombination through QDs (R_{QD}) is the predominant carrier loss process compared to recombination in the barrier (R_{bulk}). R_{bulk} is dominated by the SRH recombination, and it is slightly affected by the introduction of the QDs, since these change the bulk carrier distribution and the electric field profile already at thermal equilibrium [21]. At short circuit, the *exciton dynamics* case features recombination loss in the QDs one order of magnitude larger than the *separate e-h dynamics* case, thus causing the observed degradation of J_{sc}. The impairment of the achievable J_{sc} is also coupled to a significant degradation of the V_{oc}.

Finally, looking at the external quantum efficiency (EQE) spectra in Fig. 5, we may observe nearly identical collection efficiency of bulk photogenerated carriers between the reference cell and the QDSC one under the *separate e-h dynamics* hypothesis. In contrast, the EQE of the QD sample under the *exciton dynamics* hypothesis demonstrates degradation of the collection efficiency throughout all the wavelength spectrum. In the first case, the QDSC J_{sc} is the result of a spectral additivity between the GaAs and the QD photogeneration, while in the second case the obtained J_{sc} results from a balance between the QD induced recombination loss of bulk photogenerated

TABLE I

SUMMARY OF SIMULATED J-V CHARACTERISTICS.

	J_{sc} [mA/cm^2]	J_{sc}^{QD} [mA/cm^2]	ΔJ_{sc}, [mA/cm^2]	V_{oc} [V]
reference cell	18.75	—	—	0.91
QDSC, *separate e/h dynamics*	19.3	0.62	0.55	0.83
QDSC, *exciton dynamics*	17.8	0.55	-0.95	0.63

carriers and extended light harvesting. Additive effects on J_{sc} have been measured for example in [2,22] in line with the results obtained with the *separate e-h dynamics* model, whereas a non-additive behaviour more similar to the one predicted by the *exciton model* has been reported in [5].

The above results show that in the *separate e-h dynamics* case, despite the slow electron dynamics, high collection efficiency is possible thanks to the fast dynamics of holes, as further discussed in the following on the basis of a time-domain analysis. In particular, we study the transient evolution of the net escape rate from QDs, after the turn on of QD photogeneration, assuming that the QDs are placed in a depleted barrier. Time domain simulations were carried out within a simplified model wherein the spatial distribution of carriers is neglected (i.e. the drift-diffusion and Poisson equations are discarded) and the QD REs are solved by modeling the effect of the barrier transport by an equivalent sweep-out rate (see the conceptual sketch in the inset of Fig .6a) that accounts for the rate at which the photogenerated carriers escaping from the QDs to the barrier, are removed by the electric field from the QD capture region [23]. Since the most important mechanism driving the cell performance is the carrier exchange between the WL state and the barrier, we report here the REs used in the time-domain analysis (the superscripts e, h identify electrons and holes, respectively):

$$\frac{\mathrm{d}n_{\mathrm{B}}^{e,h}}{\mathrm{d}t} = -\frac{n_{\mathrm{B}}^{e,h}}{\tau_{\mathrm{cap}}^{e,h}} + \frac{n_{\mathrm{WL}}^{e,h}}{\tau_{\mathrm{esc}}^{e,h}} - \frac{n_{\mathrm{B}}^{e,h}}{\tau_{\text{sweep-out}}^{e,h}} \tag{2}$$

$$\frac{\mathrm{d}n_{\mathrm{WL}}^{e,h}}{\mathrm{d}t} = \frac{n_{\mathrm{B}}^{e,h}}{\tau_{\mathrm{cap}}^{e,h}} - \frac{n_{\mathrm{WL}}^{e,h}}{\tau_{\mathrm{esc}}^{e,h}} - R_{\text{WL,relax}}^{e,h} + G_{\text{WL,ph}} - R_{\text{WL,rec}} \tag{3}$$

where $n_{\mathrm{WL}}^{e,h}$ is the WL carrier density and $n_{\mathrm{B}}^{e,h}$ is the barrier carrier density in the capture region around the QD layer; the carrier rate equations for the ES and GS are the same as in [14]. The right hand terms in (2) represent the carrier capture from the barrier to the WL state, the carrier thermal escape from the WL to the barrier, and the carrier sweep-out, respectively. In (3), the last three terms on the right hand side account for the net carrier relaxation rate from the WL to the ES, ($R_{\text{WL,relax}}^{e,h}$, equal to the relaxation to ES minus the thermal escape from ES), the photogeneration rate in the WL ($G_{\text{WL,ph}}$), and the carrier loss due to recombination ($R_{\text{WL,rec}}$), respectively.

In Fig .6 we analyse the time evolution of the net escape, sweep-out and recombination rates in the two cases of a) sweep-out time faster than the capture one, b) sweep-out time slower than the capture one. The first case is representative of QDs placed in a region characterized by high electric field, where carriers are quickly removed by drift, as typically is under short circuit operation for (the most of) QDs placed in the base. The second case is representative of forward bias operation, due to the reduction of the electric field, and of QDs placed close to the highly doped contact regions (wherein carrier injection flatten the quasi-Fermi levels, thus reducing the average carrier velocity). As shown in Fig. 6(a), when the sweep-out rate is assumed faster than the capture rate, photogenerated holes (escaping out of the QDs faster than the electrons) are quickly removed from the QD region. As a consequence, only a small fraction of holes remains around the QDs and can be re-captured in the QDs. It turns out that the QDs are almost empty of holes and the slower WL electrons find no holes to recombine with. For this reason carrier recombination inside the QDs is negligible and at steady state ($t > 10\mu$s in Fig. 6a) the

net escape rate out of the QDs for both electrons and holes approaches the photogeneration rate. Therefore, in short circuit, all the QD photogenerated pairs will escape out of the QDs and will contribute to the cell current; in the same way, carriers photogenerated in the GaAs barrier and captured in the QDs will not be lost thanks to the hole fast escape. On the contrary, as shown in Fig. 6b, when the sweep-out rate gets smaller, the holes accumulated in the barrier are not removed fast enough, holes are recaptured in the QDs, quickly relax to the GS and finally recombine with electrons; in this case the dominant recombination is indeed in the GS. The steady state condition ($t > 150\mu$s in Fig. 6b) shows that the sweep-out rates of electrons and holes approach a value of about half of the photogeneration rate, whereas the rest of the photogenerated e-h pairs are lost by recombination in the QDs. This explains the reduction of the QD contribution to the photocurrent as the voltage increases as well as it evidences the main cause of the $V_{\rm oc}$ degradation: when the hole sweep-out rate decreases and becomes comparable to the hole capture, barrier (photogenerated) holes will be re-captured in the QDs promoting the recombination of photogenerated (barrier) electrons, i.e. QDs turn into recombination centers for bulk photogenerated carriers. In summary, this qualitative analysis highlights that the bulk sweep-out rate (that depends on the competition between the carrier drift driven by the electric field and the carrier diffusion from the contacts) is the key parameter that controls the QD capacity of enhancing the cell current.

Taking advantage of physics-based simulations, we can evaluate the detailed behavior of each QD layer depending on its position across the cell. Fig. 7 compares the spatial distribution of photogeneration, net escape and recombination at short circuit and full sunlight, for the *separate e-h* and the *exciton* dynamics models. It turns out that QDs placed in the middle of the intrinsic region (almost depleted of carriers and characterized by a high electric field) show efficient extraction of photogenerated carriers in both cases, albeit an increase of recombination through QDs is observed in the *exciton* case. On the other hand, the very difference appears in the QDs placed near the highly doped regions: here, under the *exciton* hypothesis, the slower hole dynamics turns QDs into efficient traps for the bulk photogenerated carriers. In fact, the holes photogenerated in the QDs or captured from the bulk can escape the QDs with a slow time constant of hundreds of picoseconds (the same as the electrons) and the escape process competes with the recombination process occurring on a similar time scale. As a consequence, we observe an increase (with respect to the *separate e-h dynamics* model) of hole population in the QDs of at least two order of magnitude throughout all the base: at the p-side QDs are filled by holes diffusing from the contact causing recombination of bulk photogenerated electrons; at the n-side the electron filled QDs easily capture and recombine the bulk photogenerated holes. Obviously the more critical layers, in terms of degradation of collection efficiency, will be those close to the illuminated emitter layers, where photogeneration is higher. Thus, the EQE in Fig. 5 shows a penalty across the whole GaAs spectrum, with larger degradation in the shorter wavelength range ($\lambda < 700$ nm), which is dominated by the layers closer to the p-emitter. The overall picture suggests that for the analyzed devices, QD doping may be expected to cause a degradation of the short-circuit current density, more significant for p-type doping than for n-type doping, in agreement with experimental results in [2] [4].

IV. Conclusions

We have discussed how the intersubband electron and hole dynamics affect the QDSC performance in terms of $J_{\rm sc}$ improvement and $V_{\rm oc}$ degradation. We have shown that the hypothesis of independent dynamics for electrons and holes (with holes faster than the electrons) predicts improved $J_{\rm sc}$, thanks to the efficient contribution of the QD layers, in line with the experimental results reported e.g. in [2,22]. On the contrary, the hypothesis that the hole dynamics mirrors the electron dynamics predicts a significant degradation of both J_{sc} and V_{oc} due to the inclusion of the QD layers, in line with the experimental results reported in [5] for undoped QDSC. These examples demonstrate the importance of quantifying the QD intersubband dynamics in the cell under forward bias and various illumination conditions. This understanding may also turn useful to find out how the doping of the intrinsic region or of the QDs can tailor the cell efficiency via modification of the carrier dynamics.

References

[1] C. G. Bailey, D. V. Forbes, S. J. Polly, Z. S. Bittner, Y. Dai, C. Mackos, R. P. Raffaelle, and S. M. Hubbard, "Open-circuit voltage improvement of InAs-GaAs quantum-dot solar cells using reduced InAs coverage," *IEEE J. Photovoltaics*, vol. 2, no. 3, pp. 269–275, July 2012.

[2] S. Polly, D. Forbes, K. Driscoll, S. Hellstrom, and S. Hubbard, "Delta-doping effects on quantum-dot solar cells," *IEEE J. Photovoltaics*, vol. 4, no. 4, pp. 1079–10 857, 2014.

[3] T. Morioka, O. Ryuji, A. Takata, Y. Shoji, T. Inoue, T. Kita, and Y. Okada, "Multi-stacked InAs/GaNAs quantum dots with direct Si doping for use in intermediate band solar cell," in *Photovoltaic Specialists Conference (PVSC) 35th IEEE*, 2010, pp. 001 834–001 837.

[4] P. Lam, S. Hatch, J. Wu, M. Tang, V. G. Dorogan, Y. I. Mazur, G. J. Salamo, I. Ramiro, A. Seeds, and H. Liu, "Voltage recovery in charged InAs/GaAs quantum dot solar cells," *Nano Energy*, vol. 6, pp. 159 – 166, 2014.

[5] A. Sablon, J. W. Little, V. Mitin, A. Sergeev, N. Vagidov, and K. Reinhardt, "Strong enhamcement of solar cell efficiency due to quantum dots with built-in charge," *Nano Letters*, vol. 11, pp. 2311–2317, 2011.

[6] K. Lüdge and E. Schöll, "Nonlinear dynamics of doped semiconductor quantum dot lasers," *The European Physical Journal D*, vol. 58, no. 1, pp. 167–174, 2010.

[7] P. Borri, S. Schneider, W. Langbein, and D. Bimberg, "Ultrafast carrier dynamics in InGaAs quantum dot materials and devices," *Journal of Optics A: Pure and Applied Optics*, vol. 8, no. 4, p. S33, 2006.

[8] T. R. Nielsen, P. Gartner, and F. Jahnke, "Many-body theory of carrier capture and relaxation in semiconductor quantum-dot lasers," *Phys. Rev. B*, vol. 69, p. 235314, Jun 2004.

[9] Y. Dai, S. Polly, S. Hellström, K. Driscol, D. Forbes, S. M. Hubbard, P. J. Roland, and R. J. Ellingson, "Effects of electric field on thermal and tunneling carrier escape in InAs/GaAs quantum dot solar cells," in *Proc. SPIE*, vol. 8981, 2014, pp. 898 106–898 106–6.

[10] K. Lüdge and E. Schöll, "Quantum-dot lasers-desynchronized nonlinear dynamics of electrons and holes," *IEEE J. Quantum Electron.*, vol. 45, no. 11, pp. 1396–1403, Nov 2009.

[11] I. Magnusdottir, A. V. Uskov, S. Bischoff, B. Tromborg, and J. Mrk, "One- and two-phonon capture processes in quantum dots," *J. Appl. Phys.*, vol. 92, no. 10, pp. 5982–5990, 2002.

[12] I. V. Ignatiev and I. E. Kozin, *Semiconductor Quantum Dots*. Berlin: Springer-Verlag, 2002, ch. Dynamics of Carrier Relaxation in Self-Assembled Quantum Dots.

[13] A. Fiore and A. Markus, "Differential gain and gain compression in quantum-dot lasers," *IEEE J. Quantum Electron.*, vol. 43, no. 4, pp. 287–294, April 2007.

[14] M. Gioannini, A. Cedola, N. Di Santo, F. Bertazzi, and F. Cappelluti, "Simulation of quantum dot solar cells including carrier intersubband dynamics and transport," *IEEE J. Photovoltaics*, vol. 3, no. 4, pp. 1271–1278, Oct 2013.

[15] G. Jolley, L. Fu, H. Lu, H. H. Tan, and C. Jagadish, "The role of intersubband optical transitions on the electrical properties of InGaAs/GaAs quantum dot solar cells," *Prog. Photovolt: Res. Appl.*, 2012.

[16] Y. Dai, C. G. Bailey, C. Kerestes, D. Forbes, and . S. M. Hubbard, "Investigation of carrier escape mechanism in InAs/GaAs quantum dot solar cells," in *Photovoltaic Specialists Conference (PVSC), 38th IEEE*, 2012, pp. 000 039–000 044.

[17] D. M. Caughey and R. E. Thomas, "Carrier mobility in Silicon empirically related to doping and field," in *Proc. IEEE*, vol. 55, 1967, pp. 2192–2193.

[18] NSM Electronic Archive: New Semiconductor Materials, Characteristics and Properties. Ioffe Physico-Technical Institute. [Online]. Available: http://www.ioffe.ru/SVA/NSM/Semicond

[19] I. O'Driscoll, T. Piwonski, C. F. Schleussner, J. Houlihan, G. Huyet, and R. Manning, "Electron and hole dynamics of InAs/GaAs quantum dot semiconductor optical amplifiers," *Appl. Phys. Lett.*, vol. 91, no. 7, pp. 071 111–071 111–3, Aug 2007.

[20] B. Lingnau, K. Lüdge, W. W. Chow, and E. Schöll, "Influencing modulation properties of quantum-dot semiconductor lasers by carrier lifetime engineering," *Appl. Phys. Lett.*, vol. 101, no. 13, p. 131107, 2012.

[21] B. Ridley, "Space-charge-mediated capture of electrons and holes in a quantum well," *Phys. Rev. B*, vol. 50, no. 3, p. 1717, 1994.

[22] D. Guimard, R. Morihara, D. Bordel, K. Tanabe, Y. Wakayama, M. Nishioka, and Y. Arakawa, "Fabrication of InAs/GaAs quantum dot solar cells with enhanced photocurrent and without degradation of open circuit voltage," *Appl. Phys. Lett.*, vol. 96, no. 20, p. 203507, 2010.

[23] M. Rossetti, P. Bardella, and I. Montrosset, "Time-domain travelling-wave model for quantum dot passively mode-locked lasers," *IEEE J. Quantum Electron.*, vol. 47, no. 2, pp. 139–150, Feb 2011.

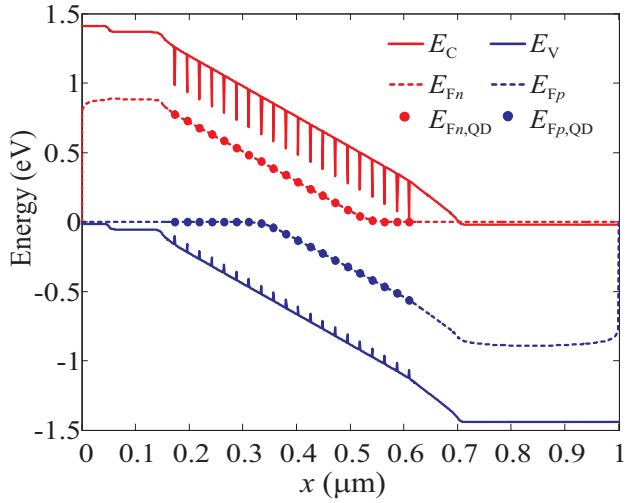

Fig. 2. Calculated energy band diagram at V=0 under 1-sun AM1.5G illumination. The QD quasi-Fermi levels ($E_{\mathrm{F}n,\mathrm{QD}}$,$E_{\mathrm{F}p,\mathrm{QD}}$) refer to the WL state.

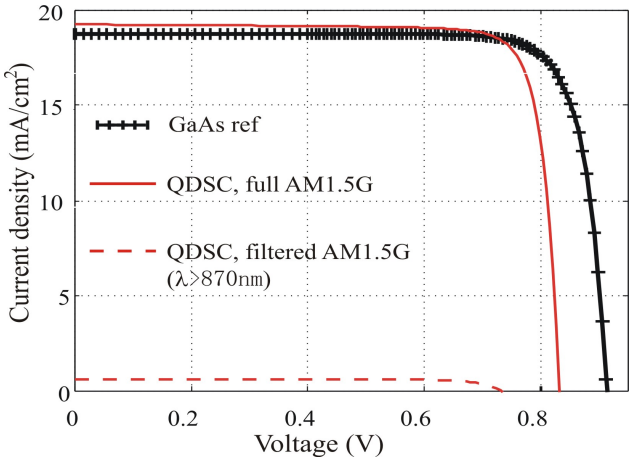

Fig. 3. Simulated J-V characteristics of the QDSC assuming *separate e-h dynamics*, under full AM1.5G illumination (solid line) and under filtered (λ >870) illumination. The J-V of the reference cell is also shown, highlighting the almost perfect spectral additivity of bulk and QD currents at short-circuit.

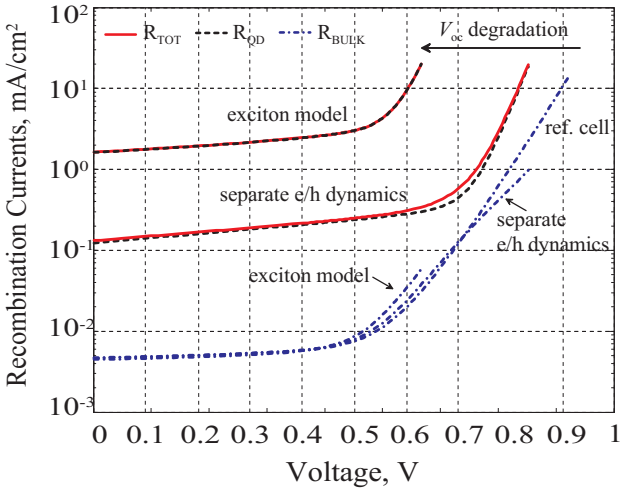

Fig. 4. Integrated recombination rates across the intrinsic region as a function of the bias voltage: black dashed line is the recombination in the QD layers, the blue dash-dot line is the SRH recombination in the bulk, and red solid line is the total.

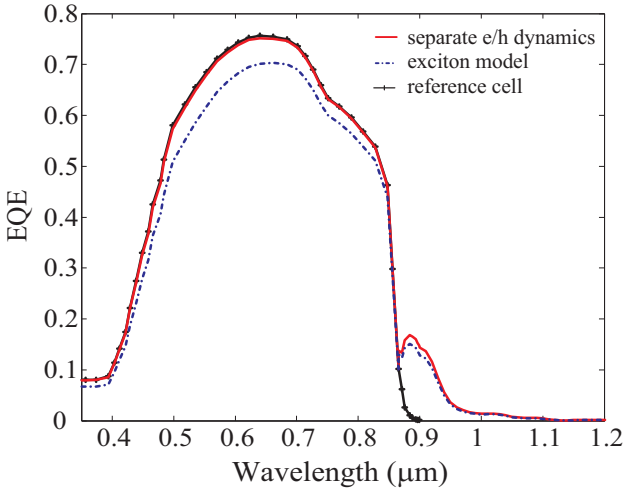

Fig. 5. Calculated EQE spectra of reference cell and QDSC cell for both the *separate e-h dynamics* model and the *exciton* model.

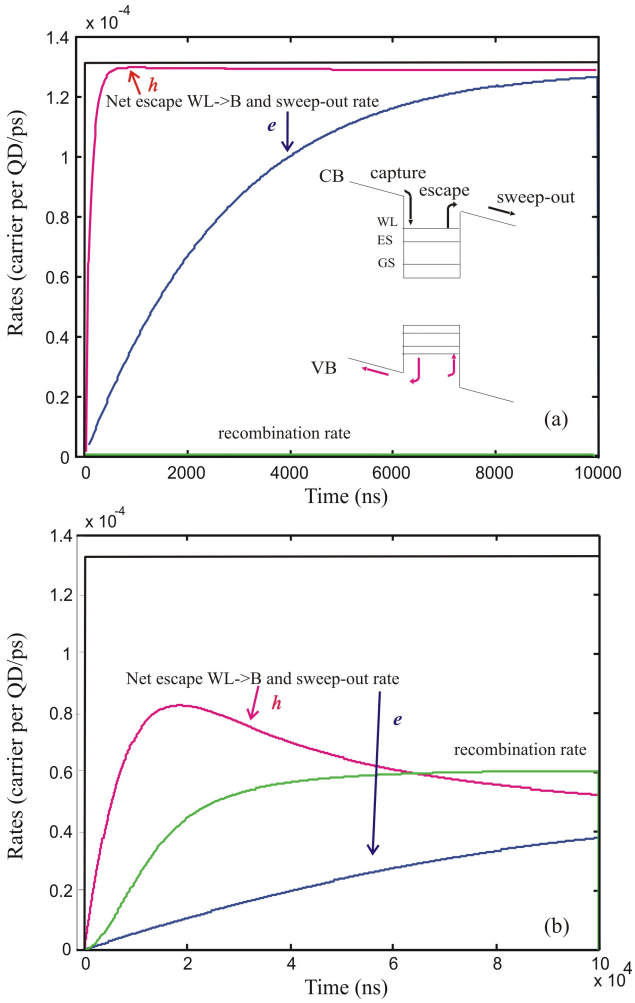

Fig. 6. Time domain analysis of the escape rate from the QDs, sweep-out and recombination rates after the turn-on of QD illumination at $t = 0$. The analysis is done by considering (a) sweep-out time faster than the capture time: $\tau^{e,h}_{\text{sweep-out}}/\tau^{e,h}_{\text{cap}} = 0.1$ and (b) sweep-out time slower than the capture time: $\tau^{e,h}_{\text{sweep-out}}/\tau^{e,h}_{\text{cap}} = 100$. The photogeneration rate is indicated by the black line; the red and blue lines indicate the net escape rate of electrons and holes from the WL to the barrier (i.e. $n^{e,h}_{\text{WL}}/\tau^{e,h}_{\text{esc}} - n^{e,h}_{\text{B}}/\tau^{e,h}_{\text{cap}}$). Notice that the net escape rates overlap with the sweep-out rates ($n^{e,h}_{\text{B}}/\tau^{e,h}_{\text{sweep-out}}$). The green line is the total recombination rate calculated as the sum of the recombination in the WL, ES and GS. For the case in (b) this rate is dominated by GS recombination.

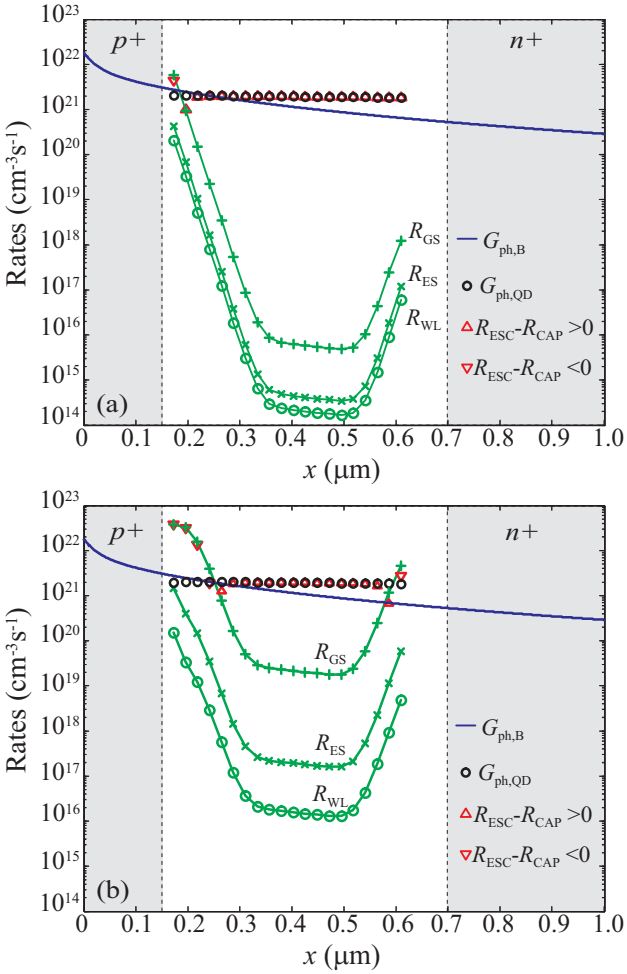

Fig. 7. Spatial distribution of bulk photogeneration (blue line) and QD photogeneration (black circles), net escape ($R_{\mathrm{ESC}} - R_{\mathrm{CAP}} > 0$ red upside triangles, $R_{\mathrm{ESC}} - R_{\mathrm{CAP}} < 0$ red downside triangles), and recombination rates through the QD states (R_{GS} R_{ES} R_{WS}, green symbols) for the *separate e-h dynamics* model (a) and for the *excitonic* model (b). Volumic rates for QD states correspond to surface rates normalized by 1 nm.